Chinese Chemical Letters 32 (2021) 425–428

Contents lists available at ScienceDirect

Chinese Chemical Letters

journal homepage: www.elsevier.com/locate/cclet

Communication

Orientation effects on C2(5)-C2′(5′) linked bioxazole isomers synthesized *via* regioselective and sequential C—H arylation

Qiang Guo[a], Li Tao[a], Chuanqi Liu[a], Xiaoyun Zhao[a], Danyang Wan[b], Jincheng Zhang[a], Jianping Ai[a], Jie Li[a,c,*]

[a] College of Optoelectronic Engineering, Chengdu University of Information Technology, Chengdu 610225, China
[b] Optical and Electrical Material Center, Xi'an Modern Chemistry Research Institute, Xi'an 710065, China
[c] National Engineering Research Center for Domestic and Building Ceramics, Jingdezhen Ceramic Institute, Jingdezhen 333403, China

ARTICLE INFO

Article history:
Received 5 April 2020
Received in revised form 29 April 2020
Accepted 9 May 2020
Available online 19 May 2020

Keywords:
Bioxazole isomers
Palladium-catalyzed
C—H arylation
Orientation effects
Photophysical properties
Theoretical calculation

ABSTRACT

Bis(4-fluorophenyl) substituted oxazole (2,5-Oxz) and C2(5)-C2′(5′) linked bioxazole isomers (C2-C2′_BOxz, C2-C5′_BOxz and C5-C5′_BOxz) were concisely synthesized *via* palladium-catalyzed regioselective and sequential C—H arylation in 1–3 reaction steps along with 20%–83% of total yields from oxazole and 4-bromofluorobenzene. The linking orientation plays a key role in the packing geometry and photophysical properties of C2-C2'_BOxz, C2-C5'_BOxz and C5-C5'_BOxz. These bioxazole isomers in solid state showed significant differences in photoluminescence quantum yields (PLQY) (0.33, 0.25 and 0.04, respectively), delayed fluorescence properties and powder X-ray diffraction (PXRD) patterns, suggesting the divergence in intermolecular interactions. The theoretically calculated gradient isosurfaces and complexation energies indicate the existence of intense π-π interactions between molecular layers, which are in good agreement with the variation trend of optical properties.

Organic semiconductor materials have been widely applied in various fields, such as organic light-emitting diodes (OLEDs), organic field-effect transistors (OFETs), organic photovoltaic (OPV) devices and sensors [1–4]. They will be important components for the next-generation displays and wearable electronic devices owing to their distinct advantages, such as lightweight, flexibility and the modifiable molecular structures along with tunable optical and electronic properties. 1,3-Azoles-based materials (oxazole, thiazole and imidazole) have been applied to high-performance organic electronic devices up to now [5–7]. Although having similar geometry as thiophene, furan and pyrrole, 1,3-azoles are widely introduced into π-conjugated semiconductors aiming at altering molecular orbital energy levels and controlling film state morphology, owing to the weak electron-withdrawing behavior, good ambient stability and large polarity [7]. Biazoles, consisting of two asymmetric azoles, have different site linked orientation (mainly C2–C2′, C2–C5′ and C5–C5′) in the molecular backbone, which could cause distinctly different photoelectric properties [8–10]. Therefore, further research about orientation effects on biazoles will promote extensive applications of azoles. However, as far as we know, few published studies about the orientation effects on bioxazole isomers (C2–C2′, C2–C5′ and C5–C5′) have been reported, mainly due to the challenges in synthesizing biazole-based building blocks [9], especially for synthesizing the bioxazole isomers in concise methods. Conventionally, the bioxazole-based derivatives were synthesized *via* the cyclization of amides or coupling of organometallic reagents [11–13], with drawbacks of lengthy synthesis steps and limited range of substrate scope, which would entail barriers for further research and applications of bioxazole derivatives.

In recent years, transition-metal-catalyzed C—H direct arylations of non-prefunctionalized (hetero)arenes have been efficient and concise routes to construct π-conjugated small molecules, oligomers and polymers [14,15]. Through the C—H direct arylation using specific C—H bonds of (hetero)arenes as functional groups, the requirement of preparing organometallic reagents and formation of organometallic salt as by-product in classical coupling methods can be avoided. Additionally, owing to the electron-withdrawing nature of C=N and electron-donating nature of heteroatom (O, S or N) in azoles, the C—H bonds on C2, C4 and C5 positions show diverse chemical activation. As a consequence, the site-selective arylation of azoles at C2 or C5 position are able to be controlled depending on the reaction conditions [16,17]. Considering the potential applications of

* Corresponding author.
E-mail address: lijie@cuit.edu.cn (J. Li).

https://doi.org/10.1016/j.cclet.2020.05.010
1001-8417/

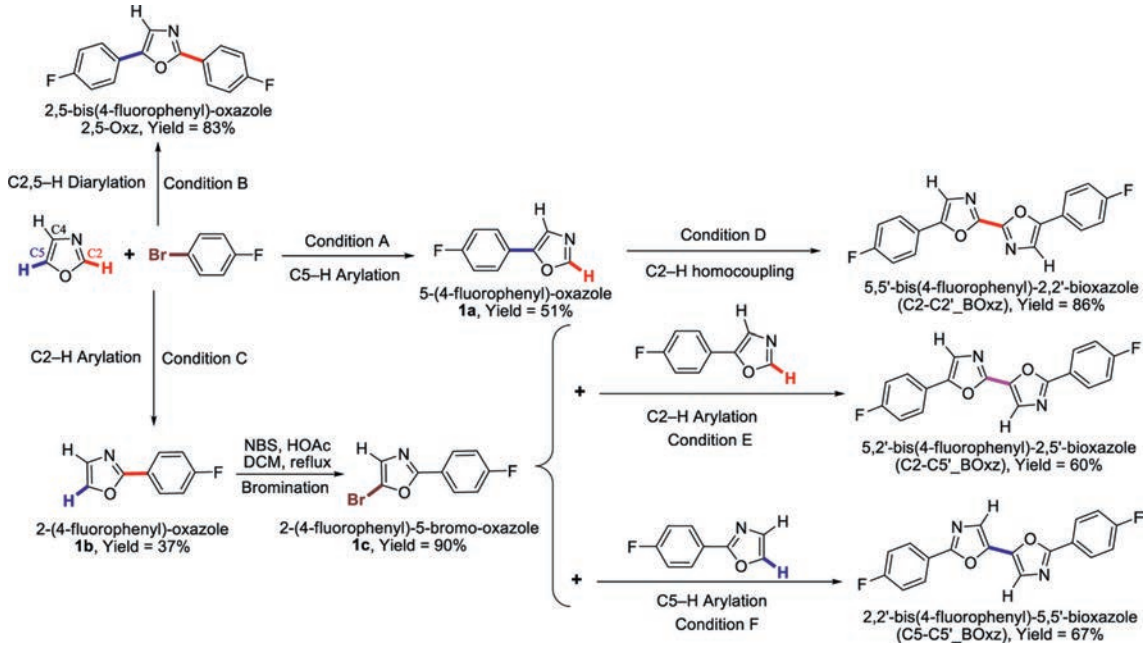

Scheme 1. Synthetic routes to biarylated oxazole and bioxazole isomers *via* regioselective and sequential C–H arylation. Condition A: 4-Bromofluorobenzene (4.0 mmol), oxazole (2.0 equiv.), $Pd(OAc)_2$ (5 mol%), butyldi-1-adamantylphosphine (10 mol%), K_2CO_3 (3.0 equiv.), PivOH (0.4 equiv.) in DMA (15 mL) at 110 °C for 24 h. Condition B: 4-Bromofluorobenzene (4.0 mmol), oxazole (2.0 equiv.), $Pd(OAc)_2$ (5 mol%), RuPhos (10 mol%), K_2CO_3 (3.0 equiv.), PivOH (0.4 equiv.) in xylene (15 mL) at 110 °C for 24 h. Condition C: 4-Bromofluorobenzene (4.0 mmol.), oxazole (2.0 equiv.), $Pd(acac)_2$ (2.5 mol%), Cs_2CO_3 (3.0 equiv.), in DMA (15 mL) at 100 °C for 16 h. Condition D: **1a** (1.0 mmol), $Pd(OAc)_2$ (10 mol%), CuCl (20 mol%), $Cu(OAc)_2$ (0.75 equiv.) in 1,4-dioxane/DMSO (v:v = 10:1, 4.4 mL), at 120 °C for 1 h. Condition E: **1a** (1.0 mmol), **1c** (1.0 mmol), $Pd(acac)_2$ (10 mol%), Cs_2CO_3 (3.0 equiv.) in DMA (4 mL) at 110 °C for 24 h. Condition F: **1b** (1.0 mmol), **1c** (1.0 mmol), $Pd(OAc)_2$ (10 mol%), KOAc (2.0 equiv.) in DMA (4 mL) at 110 °C for 24 h.

bioxazole derivatives and the advantages C—F of C—H arylation, we herein presented a straightforward and concise way to synthesize 2,5-biarylated oxazole and bioxazole isomers (C2–C2′, C2–C5′ and C5–C5′ linked orientation) *via* palladium-catalyzed regioselective and sequential C—H arylation. Under appropriate reaction conditions, the 4-fluorophenyl substituted (bi)oxazole isomers can be obtained in only 1–3 reaction steps with 20%–83% of total yields. And the orientation effects on these isomers were also investigated by experimental and computational analysis.

Fluorinated organic materials have gained great interest in the area of organic electronics, because of the strong electronegativity of fluorine atom, weak C—F···π interaction [18] and further derivatization *via* C—F bond activation [19]. Therefore, 4-fluorophenyl bioxazole isomers were chosen as our research objects. During the past decade, many efforts have already been done to overcome the challenges in C—H arylation of oxazoles [20–25]. Among them, Strotman *et al.* [24] and Shi *et al.* [25] have successfully realized the regiodivergent arylation (C2- *vs.* C5-arylations) of unsubstituted oxazole under their optimized palladium-catalyzed reaction conditions with or without phosphine ligands, respectively. As shown in Scheme 1, employing 4-bromofluorobenzene (1.0 equiv.) and oxazole (2.0 equiv.) as sources, C5-monoarylated oxazole (**1a**, 5-(4-fluorophenyl)-oxazole) was obtained in moderate yield (51%) in the presence of $Pd(OAc)_2$ (5 mol%), butyldi(1-adamantyl)-phosphine (10 mol%), K_2CO_3 (3.0 equiv.), PivOH (0.4 equiv.) in *N,N*-dimethylacetamide (DMA, 15 mL) at 110 °C for 24 h, (Scheme 1, condition A). Unhappily, only 2,5-diarylated oxazole (2,5-bis(4-fluorophenyl)-oxazole, abbreviated as 2,5-Oxz) was obtained in good yield (83%) instead of the desired C2-monoarylated product under condition B. When choosing a new catalytic system, 5 mol% of $Pd(acac)_2$, 3 equiv. of Cs_2CO_3, in DMA at 110 °C for 24 h, a mixture of C2-monoarylated oxazole (**1b**, 2-(4-fluorophenyl)-oxazole) and 2,5-diarylated oxazole (2,5-Oxz) was detected. Obviously, the C5-arylation of formed 2-(4-fluorophenyl)-oxazole and C2-arylation of oxazole are competitive reactions under condition B. Because the activation energy of C—H bond at C5-position of oxazole is lower than that at C2-positon, the arylation of C5–H bond is always preferred in palladium-catalyzed concerted metalation-deprotonation (CMD) pathway [16]. To increase the ratio of **1b**:2,5-Oxz and suppress C5-arylation of **1b**, the reaction condition was modified slightly. After reducing catalyst $Pd(acac)_2$ loading to 2.5 mol%, lowering reaction temperature to 100 °C and shorting reaction time to 16 h (condition C), **1b** was successfully obtained in 37% of isolated yield.

With C2- and C5-monoarylated oxazole isomers (**1a** and **1b)** in hand, we began to explore methods to construct bioxazole isomers. The 2,2'-bioxazole isomer (C2-C2'_BOxz), was synthesized *via* a straightforward and atom-economic way, oxidative C2–H homocoupling of **1a**. A mixture of **1a** (1.0 equiv.), $Pd(OAc)_2$ (10 mol%), CuCl (20 mol%), $Cu(OAc)_2$ (0.75 equiv.) dissolved in 1,4-dioxane/DMSO (10:1, v/v) was heating at 120 °C for 1 h (Scheme 1, condition D) [26], and the reaction run smoothly to form C2-C2'_BOxz in good yield (86%). After bromination of **1b** at C5 position, brominated product **1c** was undergoing C—H/C–Br type direct arylation with **1a** and **1b** to afford C2-C5'_BOxz (yield = 60%) and C5-C5'_BOxz (67% yield) under condition E and condition F, respectively (Scheme 1). Under our synthetic strategy, 2,5-biarylated oxazole (2,5-Oxz) and bioxazole isomers (C2-C2'_BOxz, C2-C5'_BOxz and C5-C5'_BOxz) can be successfully obtained *via* palladium-catalyzed sequential C—H arylation in only 1–3 reaction steps along with total yields of 20%–83% from commercially available sources. It is worth noting that the substituent groups or coupling position of (bi)oxazoles are

Table 1
Experimental and calculated optical properties of 2,5-biarylated oxazole and bioxazole isomers.

Compound	Experimental data						Calculated data[e]			
	Solution[a]			Film[b]			Solution			
	$\lambda_{max,abs}$ (nm)	$\lambda_{max,PL}$[c] (nm)	PLQY[d]	$\lambda_{max,abs}$ (nm)	$\lambda_{max,PL}$[c] (nm)	PLQY[d]	$\lambda_{max,abs}$ (nm)	$\lambda_{max,PL}$ (nm)	k_r (s^{-1})	k_{nr} (s^{-1})
2,5-Oxz	303	363	0.69	305	362	0.11	302	358	4.94×10^8	3.76×10^4
C2-C2'_BOxz	334	399	0.77	335	422	0.33	327	396	5.50×10^8	4.58×10^4
C2-C5'_BOxz	332	399	0.72	334	439	0.25	326	393	5.42×10^8	3.11×10^4
C5-C5'_BOxz	328	395	0.75	328	447	0.04	327	394	5.37×10^8	8.80×10^5

[a] In dilute toluene solution (2×10^{-5} mol/L), abs = absorption, PL = photoluminescence.
[b] 10 wt% (bis)oxazole : polystyrene (PS) doped film.
[c] Excited at the corresponding maximum absorption wavelength.
[d] Absolute quantum yield.
[e] Calculated by Gaussian 16 package and MOMAP program.

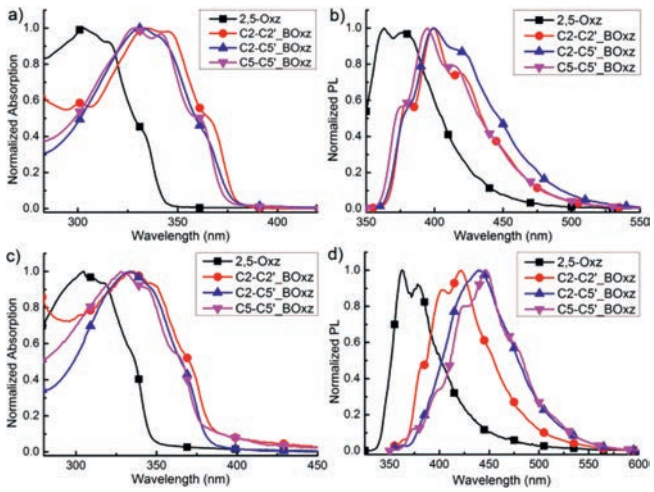

Fig. 1. Normalized UV–vis absorption (a for solutions and c for films) and photoluminescence (b for solutions and d for films) spectra of 2,5-Oxz, C2-C2'_BOxz, C2-C5'_BOxz and C5-C5'_BOxz.

able to be programed owing to the feasibility of regioselective arylation of oxazoles.

Subsequently, as summarized in Table 1 and Fig. 1, optical properties of 2,5-biarylated oxazole (2,5-Oxz) and bioxazole isomers (C2-C2'_BOxz, C2-C5'_BOxz and C5-C5'_BOxz) were characterized. All four compounds show very similar absorption in the near-ultraviolet (UV) region ($\lambda_{max,abs}$ = 303, 334, 332, 328 nm in toluene and 305, 335, 334, 328 nm in doped films, respectively) and various photoluminescence in the near-UV-blue region ($\lambda_{max,PL}$ = 363, 399, 399, 395 nm in toluene and 362, 422, 439, 447 nm in doped films, respectively). Meanwhile, the photoluminescence quantum yields (PLQY) of them in doped films drastically decrease as compared to that in toluene. In contrast with that of bioxazole isomers, mono-oxazole derivative (2,5-Oxz) shows obvious blue-shift in absorption and photoluminescence spectra, owing to its less π-conjugation. The close resemblance of absorption spectra of the three bioxazole isomers both in toluene solution and in thin films states indicate that they have similar ground states. On the contrary, the photoluminescence spectra of bioxazole isomers in film states are different from each other. The maximum emission wavelengths of C5-C5'_BOxz ($\lambda_{max,PL}$ = 447 nm) and C2-C5'_BOxz ($\lambda_{max,PL}$ = 439 nm) in film state show obvious red-shift comparing with that of C2-C2'_BOxz ($\lambda_{max,PL}$ = 422 nm). We speculate that C5-C5'_BOxz and C2-C5'_BOxz show stronger intermolecular interaction than C2-C2'_BOxz in solid state, because strong intermolecular interaction usually results in a spectral red-shift [27]. Meanwhile, the PLQY of C5-C5'_BOxz in film state (0.04) is much lower than that of the other two isomers (0.25 for C2-C5'_BOxz and 0.33 for C2-C2'_BOxz). In order to clarify the intermolecular interactions more clearly, transient PL decay characteristics and powder X-ray diffraction (PXRD) of these compounds were measured (Figs. S1-S4 and Table S1 in Supporting information). All the bioxazole isomers in solution show only one prompt component with emission lifetimes about 1.20–1.38 ns. On the contrary, all of them in doped films exhibit two decay components, suggesting the existence of intermolecular interaction [28]. Compared with C2-C2'_BOxz and C2-C5'_BOxz, C5-C5'_BOxz possesses the most distinctive delayed feature with emission lifetime about 9.4 μs, which indicates that C5-C5'_BOxz has the strongest intermolecular interaction in doped film. Moreover, all the PXRD patterns presented clearly different diffraction peaks, indicating their difference in molecular packing (Fig. S4 in Supporting information) [29]. And the obvious and maximum 2θ peak position at 33.2° of C5-C5'_BOxz also illustrates the existence of a tightest *d*-spacing.

To further understand the orientation effects on these oxazole derivatives, theoretical calculations were carried out by using Gaussian 16 package [30]. Ground state geometries (S_0) of structures were fully optimized by using M06-2X hybrid functional [31] of density functional theory (DFT) with 6-311 G(d) basis set, and their lowest singlet excited state (S_1) geometries were also optimized by using time-dependent density functional theory (TD-DFT) at M06-2X/6-311 G(d) level. Additionally, the optimized geometries were further characterized by vibrational frequencies analysis to make sure all stationary points are minima (zero imaginary frequencies). TD-DFT was then employed to simulate the absorption and emission properties. The absorption, emission spectra and (non)radiative transition rates of oxazoles in toluene were performed by MOMAP program [32]. As shown in Fig. S5 (Supporting information), the calculated optical spectra are in good agreement with their experimental spectra, indicating that the M06-2X/6-311 G(d) optimized geometries are reasonable to estimate the ground state and excited state geometries. The calculated radiative transition rates ($k_r = 10^8$ s^{-1}) from S_1 to S_0 are three to four orders of magnitude higher than their corresponding nonradiative internal conversion rates ($k_{nr} = 10^{4\text{-}5}$ s^{-1}) (Table 1), suggesting that these oxazole derivatives would be good chromophores for pure blue emitters with high PLQY.

The highest occupied molecular orbital (HOMO), the lowest unoccupied molecular orbital (LUMO) and molecular electrostatic potential (ESP) were calculated with the optimized S_0 geometries (Figs. S6 and S7 in Supporting information). All four fluorophenyl oxazole derivatives have highly coplanar geometries, and the electron density of HOMO, LUMO and ESP were delocalized over the entire backbones without any conjugation breakages. Through the calculated data, all of the electronic transitions of oxazoles are of

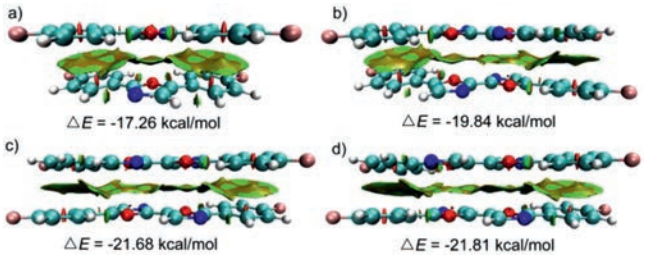

Fig. 2. Gradient isosurfaces (s = 0.5 au) for antiparallel displaced dimer of a) 2,5-Oxz, b) C2-C2'_BOxz, c) C2-C5'_BOxz and d) C5-C5'_BOxz. ΔE means BSSE corrected complexation energies of dimers; the color-mapped reduced density gradient (RDG) isosurface between dimer means π-π interaction.

the π-π^* type transition for both absorption and emission with main transition configuration of HOMO → LUMO along with giant oscillator strength (all over 1.0) (Fig. S6 and Table S2 in Supporting information). The molecular ESP of these four oxazole compounds can be seen in Fig. S7. The most negative ($V_{S,min}$) and positive ($V_{S,max}$) values of electrostatic potential on molecular surfaces [33–35], as well as the extreme values at the aromatic ring regions are significantly different, which would cause different strength of noncovalent interaction and solid morphology [36]. In addition, the complexation energies of dimers of bioxazole isomers in gas phase were also calculated to estimate the strength of noncovalent intermolecular interactions with functional and basis set of M06-2X-D3/6-311+G(d,p) [37]. The basis set superposition error (BSSE) corrected complexation energies of C2-C2'_BOxz, C2-C5'_BOxz and C5-C5'_BOxz antiparallel displaced dimers are −19.84, −21.68 and −21.81 kcal/mol, respectively. This increasing trend (absolute value) of complexation energies of bioxazole dimers indicated the increasing strength of intermolecular interaction (π-π stacking interaction, shown in Fig. 2) [38], and might be the reason for the red-shifts in the photoluminescence spectra of bioxazole isomers in film state. Similar results, stronger intermolecular interaction of 5,5'-biazoles than that of 2,2'-biazoles, can also be observed at other literature and would be beneficial for high-performance OFET [8].

In summary, we have designed and synthesized bis-(4-fluorophenyl) substituted oxazole (2,5-Oxz) and bioxazole isomers with different site linked orientation (C2-C2'_BOxz, C2-C5'_BOxz and C5-C5'_BOxz) *via* palladium-catalyzed regioselective and sequential C–H arylation. Under suitable reaction conditions, these (bi)oxazole isomers can be programed and successfully obtained in only 1–3 reaction steps along with 20%–83% of total yields from oxazole and 4-bromofluorobenzene. Then their photophysical properties including absorption, photoluminescence and PLQYs both in dilute toluene solutions and in doped films were systematically characterized. All four compounds show absorption in the near-UV region and photoluminescence in the near-UV-blue region, with high PLQY up to 0.75. The red-shift in fluorescence spectrum, low PLQY (0.04) and obvious delayed fluorescence properties of C5-C5'_BOxz in thin film and PXRD pattern in solid state indicated its close molecular packing in solid state. Moreover, theoretical calculations were further performed to analyze their electronic transitions and to predict the noncovalent intermolecular interactions. Combining the advantages of good coplanarity, large π-conjugated system, giant oscillator strength and high radiative transition rates ($k_r = 5.50 \times 10^8$ s^{-1}), C2-C2'_BOxz derivatives could be good candidate as pure blue emitters with high performance. In contrast, the close packing in solid state and strong interaction of C5-C5'_BOxz suggest its potential applications for OFET devices. This work provides a valuable strategy for synthesizing C2(5)-C2′(5′) linked bioxazole isomers as well as investigating the orientation effects on their optical properties and further applications.

Declaration of competing interest

The authors declare that they have no known competing financial interests or personal relationships that could have appeared to influence the work reported in this paper.

Acknowledgments

We gratefully thank the financial support from the National Natural Science Foundation of China (Nos. 21801028, 11704050, 61505015), Scientific Research Project of the Education Department of Sichuan Province (No. 2018Z099) and Project of Science and Technology Department of Sichuan Province (No. 2017FZ0085). We would like to thank Dr. Danyang Wan for the quantum chemical calculations in this paper.

Appendix A. Supplementary data

Supplementary material related to this article can be found, in the online version, at doi:https://doi.org/10.1016/j.cclet.2020.05.010.

References

[1] X. Zhang, H. Dong, W. Hu, Adv. Mater. 30 (2018) 1801048.
[2] J. Li, K. Pu, Chem. Soc. Rev. 48 (2019) 38–71.
[3] M. Moser, J.F. Ponder Jr., A. Wadsworth, A. Giovannitti, I. McCulloch, Adv. Funct. Mater. 29 (2019)1807033.
[4] Z. Fu, K. Wang, B. Zhou, Chin. Chem. Lett. 30 (2019) 1883–1894.
[5] V.S. Padalkar, S. Seki, Chem. Soc. Rev. 45 (2016) 169–202.
[6] W.C. Chen, Z.L. Zhu, C.S. Lee, Adv. Opt. Mater. 6 (2018) 1800258.
[7] Y. Lin, H. Fan, Y. Li, X. Zhan, Adv. Mater. 24 (2012) 3087–3106.
[8] S. Ando, R. Murakami, Ji. Nishida, et al., J. Am. Chem. Soc. 127 (2005) 14996–14997.
[9] H. Usta, W.C. Sheets, M. Denti, et al., Chem. Mater. 26 (2014) 6542–6556.
[10] K. Oniwa, H. Kikuchi, T. Kanagasekaran, et al., Chem. Commun. 52 (2016) 4926–4929.
[11] R.L. Taber, G.D. Grantham, E.S. Binkley, P.G. Grant, J. Chem. Eng. Data 18 (1973) 436–438.
[12] J. Wang, S. Luo, J. Li, Q. Zhu, Org. Chem. Front. 1 (2014) 1285–1288.
[13] J.K. Politis, F.B. Somoza Jr., J.W. Kampf, M.D. Curtis, Chem. Mater. 11 (1999) 2274–2284.
[14] K. Okamoto, J. Zhang, J.B. Housekeeper, S.R. Marder, C.K. Luscombe, Macromolecules 46 (2013) 8059–8078.
[15] Y. Segawa, T. Maekawa, K. Itami, Angew. Chem. Int. Ed. 54 (2015) 66–81.
[16] S.I. Gorelsky, Coord. Chem. Rev. 257 (2013) 153–164.
[17] C.B. Bheeter, L. Chen, J.F. Soulé, H. Doucet, Catal. Sci. Technol. 6 (2016) 2005–2049.
[18] R. Berger, G. Resnati, P. Metrangolo, E. Weber, J. Hulliger, Chem. Soc. Rev. 40 (2011) 3496–3508.
[19] T. Braun, R.P. Hughes, Organometallic Fluorine Chemistry, Springer, Cham, Switzerland, 2015.
[20] C. Verrier, P. Lassalas, L. Théveau, et al., Beilstein J. Org. Chem. 7 (2011) 1584–1601.
[21] Y. Yang, J. Lan, J. You, Chem. Rev. 117 (2017) 8787–8863.
[22] B. Li, J. Lan, D. Wu, J. You, Angew. Chem. Int. Ed. 54 (2015) 14008–14012.
[23] Z. Sipos, K. Kónya, Synlett 29 (2018) 2412–2416.
[24] N.A. Strotman, H.R. Chobanian, Y. Guo, J. He, J.E. Wilson, Org. Lett. 12 (2010) 3578–3581.
[25] X. Shi, J.F. Soulé, H. Doucet, Adv. Synth. Catal. 361 (2019) 4748–4760.
[26] J. Dong, Y. Huang, X. Qin, et al., Chem. Eur. J. 18 (2012) 6158–6162.
[27] F.C. Spano, Acc. Chem. Res. 43 (2010) 429–439.
[28] H. Fukagawa, T. Shimizu, N. Ohbe, et al., Org. Electron. 13 (2012) 1197–1203.
[29] K.D.M. Harris, P.A. Williams, Powder diffraction, in: D. Bruce, D. O'Hare, R.I. Walton (Eds.), Structure from Diffraction Methods, John Wiley and Sons Ltd, Chichester, 2014, pp. 1–74.
[30] M.J. Frisch, G.W. Trucks, H.B. Schlegel, et al., Gaussian 16, Revision A.03, Gaussian, Inc., Wallingford CT, 2016.
[31] Y. Zhao, D.G. Truhlar, Theor. Chem. Account. 120 (2008) 215–241.
[32] MOMAP - Molecular Material Property Prediction Package: http://www.momap.net.cn.
[33] T. Lu, F. Chen, J. Comput. Chem. 33 (2012) 580–592.
[34] T. Lu, F. Chen, J. Mol. Graph. Model. 38 (2012) 314–323.
[35] W. Humphrey, A. Dalke, K. Schulten, J. Mol. Graph. 14 (1996) 33–38.
[36] J.S. Murray, P. Politzer, WIREs Comput. Mol. Sci. 7 (2017) e1326.
[37] R. Sedlak, T. Janowski, M. Pitoňák, et al., J. Chem. Theory Comput. 9 (2013) 3364–3374.
[38] E.R. Johnson, S. Keinan, P. Mori-Sánchez, et al., J. Am. Chem. Soc. 132 (2010) 6498–6506.